The Microstructural Stability of a Ruptured Thermal Creep Specimen of MA957 - D.T. Hoelzer, J.P. Shingledecker, R.L. Klueh, M.K. Miller, and J. Bentley (Oak Ridge National Laboratory)

OBJECTIVE

To report the results of several creep tests that were performed on MA957 in 2003 and the results of the microstructural analysis of a specimen that failed recently after 38,555 h at 800ºC in air and a 100 MPa load. A key focus of this study was to investigate the thermal stability of the Ti-, Y-, O-enriched nanoclusters that are present in MA957 after the long exposure time at 800ºC.

SUMMARY

A set of thermal creep tests were conducted on as-received MA957 starting in August 2003 shortly after discovering a high number density of Ti-, Y-, and O-enriched nanoclusters that were similar to those that had been discovered in 12YWT by APT in 1999. Four of the creep tests that were conducted at temperatures between 875ºC and 925ºC with 70 or 100 MPa loads ended with failure of the specimens before reaching 2000 h. On the other hand, two of the creep tests were conducted at lower temperatures of 800ºC (100 MPa) and 825ºC (70 MPa) and these lasted a considerably longer time. However, the specimen that was tested at 800ºC and 100 MPa recently failed after 38,555 h while the other specimen that was tested at 825ºC and 70 MPa is still in progress with more than 43,000 h logged to date. The microstructure of the recently failed creep specimen was investigated using optical microscopy and TEM, including Energy-Filtered TEM (EFTEM). The optical microscopy and TEM results showed that extensive porosity formed throughout the microstructure during the creep test. However, the significant discovery obtained by EFTEM revealed that the nanoclusters experienced no significant change in size, indicating that they are extremely stable at 800ºC (and 100 MPa) for very long periods of time.

PROGRESS AND STATUS

Background

There has been a renewed interest in the MA957 ferritic alloy that was patented by INCO in 1978 [1] following the discovery of a high number density of Ti-, Y-, and O-enriched nanoclusters (NC) by Atom Probe Tomography (APT) [2] and Small Angle Neutron Scattering (SANS) [3] during the FY02-05 I-NERI project between ORNL, plus UCSB subcontract, and CEA, Saclay, in France. The NC were found to have similar composition to those originally discovered by APT in 12YWT [4], which was developed in Japan during the 1990's [5]. The INERI project focused on 2 main tasks: (1) investigating the microstructure, with particular interest on the NC, and mechanical properties of the benchmark MA957 and 12YWT alloys, since they were produced by commercial companies (INCO and Kobe Steel, respectively) and (2) investigating the processing parameters toward development of the experimental 14YWT alloy.

The majority of recent results pertaining to microstructural analysis and mechanical properties testing of MA957 have been conducted on a thick walled tube sample that was provided to ORNL by CEA, Saclay in 2003 during the I-NERI project. Figure 1 shows the salient microstructural characteristics of the as-received MA957. The bright-field TEM micrograph in Figure 1a shows the general grain size and morphology observed in the microstructure at low-magnification. The grain size that was measured normal to the elongated grain direction was 654 +/- 79 nm and the grain length-to-width ratio, or aspect ratio (GAR), varied from ~3 to 10. The TEM analysis also revealed the presence of stringers of micron size Al_2O_3 oxide particles and low number densities of TiO_2 and $Ti_2Y_2O_7$ oxide particles with sizes typically >~20 nm. The Atom Probe Tomography (APT) results shown in Figure 1b reveal the Ti-, Y-, and O-enriched NC that are present in the as-received MA957. The analysis of the NC using the maximum separation envelope method [6] determined that the Guinier radius was r_g = 1.2 +/- 0.4 nm, the number density was ~2 x 10^{24} m^{-3}, and the average composition was 32.9 +/- 5.3 at.% Ti, 15.4 +/- 7.3% Y, 39.9 +/- 6.9% O, 1.7 +/- 1.7% Cr, 0.02 +/- 0.2% Mo, and remaining balance of Fe. The size and number

density of the NC determined from Small Angle Neutron Scattering (SANS) was r = 1.3 nm and ND = 0.7 x 10^{24} m^{-3} [3], which was in agreement with the APT results.

Following the discovery of NC in the as-received MA957, a total of 6 creep tests were initiated in August of 2003 to compare the creep properties with those of 12YWT, which had been completed on an earlier LDRD project at ORNL. The creep tests were conducted in air at temperatures ranging from 800ºC to 925ºC with loads of either 70 or 100 MPa. Four creep tests ended with specimen failures occurring within ~68 days of tests. All of these tests were conducted at 875ºC to 925ºC. Two of the tests (800ºC and 100 MPa and 825ºC and 70 MPa) continued without failure for more than 4 years. However, the specimen tested at 800ºC failed in early January, 2008 after 38,555 h, while the other specimen tested at 825ºC is still in progress with more than 43,000 h. The main objective of this report is to present the results of the creep test and the microstructural analysis of the specimen that recently failed after 38,555 h at 800ºC and 100 MPa.

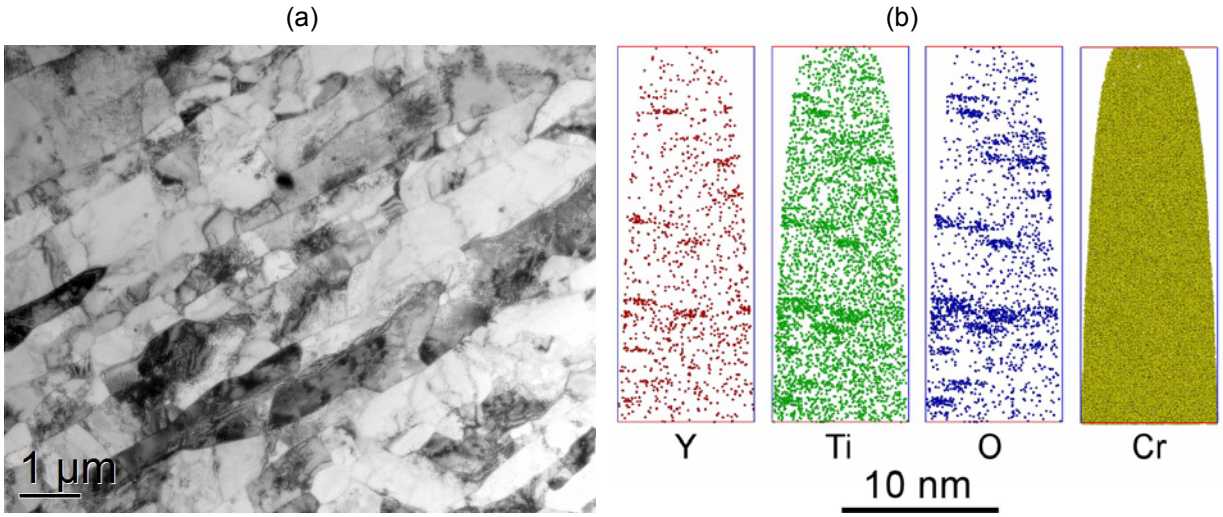

Figure 1. The as-received MA957 showing (a) bright-field TEM micrograph of the elongated grain structure and (b) APT of the Ti-, Y-, O-enriched nanoclusters including the solute Cr distribution.

Experimental Procedure

The sample of MA957 that was received in August, 2002 from CEA, Saclay consisted of a 100 mm long tube that had an external diameter of 65 mm and wall thickness of 9 mm. No information was provided on the fabrication history of this tube sample. A total of 7 creep specimens were machined from the tube wall section. The specimens were 3.0 in. long and had cylindrical gages, which were 0.8 in. long and 0.199 in. diameter. A total of 6 creep tests were started in August 2003. The temperatures and stresses used in these tests are shown in Table 1. All of the creep tests were conducted in air.

Results and Discussion

Thermal creep properties

The results of the 6 creep tests along with the test conditions are shown in Table 1. All of the specimens that were tested in the 875 to 925ºC temperature range failed within a short period of time, i.e. equivalent to ~1.5 to 68 days. At these temperatures, the protective Cr_2O_3 scale becomes unstable due to volatility of the CrO_3 phase [7] and oxidation of the specimens. These results show that lower test temperatures and stresses resulted in lower strains at failure and longer test durations. However, significantly longer time-spans resulted with the 2 specimens that were tested at the lower temperatures of 800ºC and 825ºC. As

shown in Table 1, the specimen that was tested at 800 ºC and 100 MPa recently failed after 38,555 h and the one tested at 825ºC and 70 MPa is still in progress.

Figure 2 shows the plot of the Larson-Miller Parameters (LMP) for the 6 additional creep tests conducted on MA957 and also those obtained in previous studies of the mechanically alloyed (MA) 12YWT ferritic alloy and advanced 9Cr-WMoVNb tempered martensitic steel (TMS) [7]. The 2 data points at 650ºC for MA957 were obtained from the INCO patent [1]. The temperature and time-to-failure are provided for the creep tests on 12YWT and MA957. The linear line fit through the data demonstrates that the overall creep properties of 12YWT are better than that of MA957, but both of these MA ferritic alloys show significant improvements over the 9Cr-WMoVNb TMS. The LMP data for 12YWT and MA957 are 4 to 6 orders of magnitude higher than that for the 9Cr-WMoVNb TMS at all stresses. Unfortunately, the LMP does not provide any information about the creep strain behavior and total strain at failure.

Table 1. Shows the test conditions and the results of the creep tests that were conducted on MA957.

Specimen	Stress (MPa)	Temperature (ºC)	Time (h)	Strain at Failure (%)	Status
1	100	900	37	1.8	Ruptured
2	70	925	165	4.2	Ruptured
3	70	875	1640	3.4	Ruptured
4	100	800	38,555	6.5	Ruptured
5	70	825	43,777	N/A	In Test
6	100	875	42	6.6	Ruptured

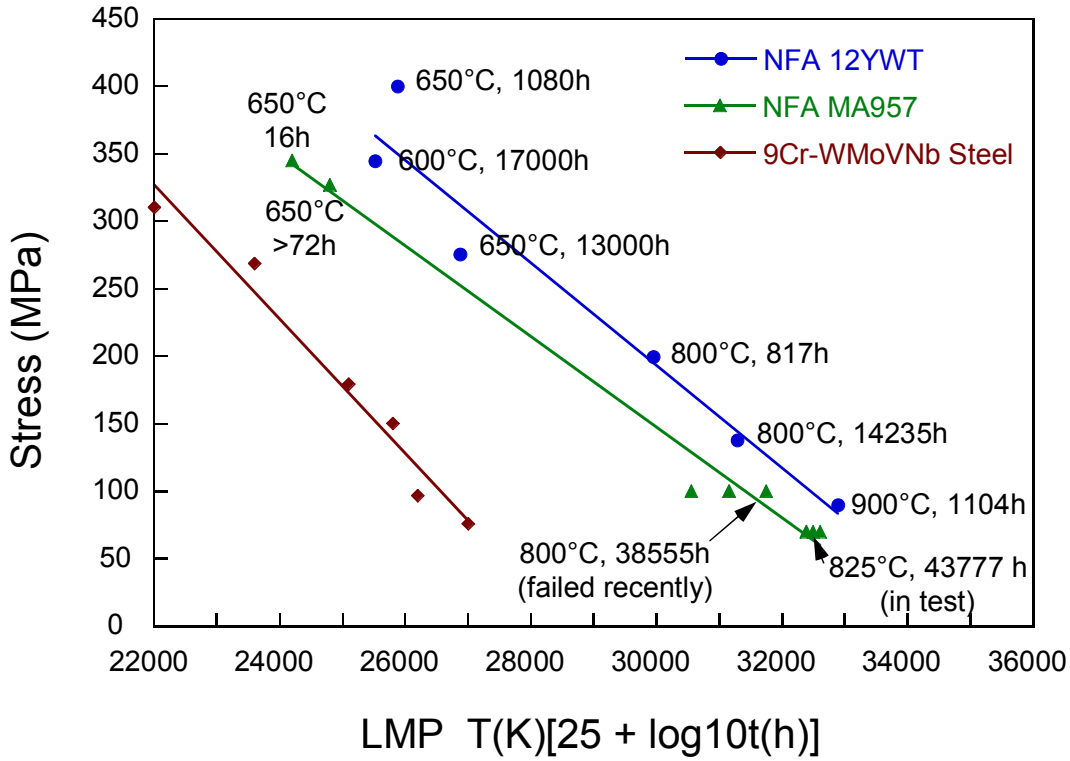

Figure 2. The Larson Miller Parameter plots of the new data for MA957 and of MA957, 12YWT and 9Cr-WMoVNb TMS from previous studies [1,7].

The results of the creep test for the specimen that failed after 38,555 h at 800ºC and 100 MPa are shown in Figure 3. This plot shows the creep strain as a function of time with the data processed to 100 points due to the very large number of data points for this test. Interestingly, the results do not show significant evidence of primary creep and tertiary creep behavior. The data follows nearly steady state creep rate from the beginning of the test to ~38,165 h. The results indicated that the vast majority of strain, ~6.14%, occurred in the last 0.1 h of the test. The extensometer creep strain prior to rupture was 0.361%, which corresponded to a displacement of ~0.003 in. for the 38,555 h test. The minimum creep rate was measured to be ~1.2 x 10^{-11} s^{-1} ($d\dot{\varepsilon}/dt$), which is a very low value.

Microstructural characterization

The digital image of the two ends of the ruptured test specimen is shown in Figure 4. The dark contrast visible on the external surface of the gages is from the oxide scale that formed during the creep test. In addition, the analysis of the fracture surfaces at the end of each gage section also showed dark contrast, which indicated that these surfaces had been exposed to the oxidizing atmosphere at 800ºC for a sufficient period of time before the specimen failed.

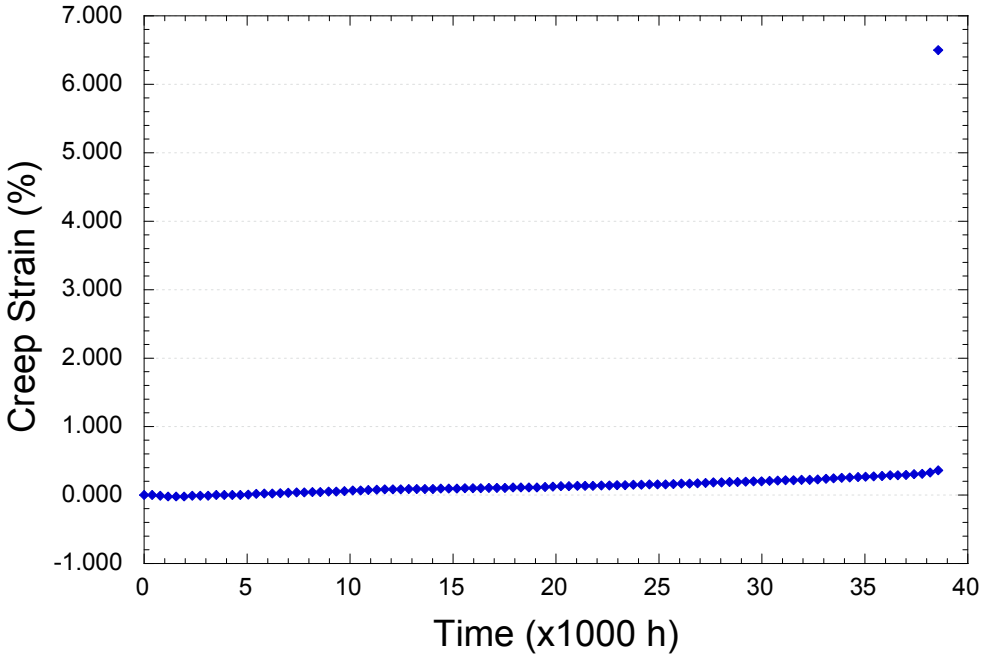

Figure 3. Results showing the creep strain as a function of time for the test conducted on the MA957 specimen at 800ºC in air and 100 MPa load.

Figure 4. Digital image showing the broken sections of the ruptured specimen of MA957.

The general microstructural investigation of the ruptured MA957 specimen was conducted using optical microscopy and transmission electron microscopy (TEM). A thin, ~1 mm thick, cylindrical-shaped sample was cut about 5 mm away from fracture surface of the longer gage section (the left gage section in Figure 4). This sample was mounted and polished for optical microscopy, and will be examined by SEM analysis in the future. Several 3 mm diameter TEM foils were prepared from another cylindrical-shaped sample that was cut from the same gage section. This sample was ~4 mm thick, which enabled the 3 mm diameter thin foil specimens to be prepared with an orientation that was parallel to the elongated grains, i.e. parallel to the gage. The foils were jet-polished in a Tenupol-3 using an electrolyte solution of 75% methanol and 25% nitric acid at 27ºC for TEM analysis.

The results of the microstructural analysis of the ruptured specimen using optical microscopy are shown in Figure 5. At low magnifications (Figure 5a), a complex surface oxide scale and extensive porosity throughout the microstructure are observed. The pores range in size from ~1 to ~20 μm and appear to be distributed in stringers. Similar porosity has been observed in other studies following exposure of ODS alloys to elevated temperatures during annealing of PM200 [9] and oxidation of ODS Fe-Cr alloys [10]. The reasons for explaining the formation of pores at high temperatures are not fully understood. Figure 5b shows the optical micrograph of the surface oxide scale at higher magnification. The surface oxide scale consists of several layers based on differences in contrast observed by optical microscopy. The outer layer varies considerably in thickness, from ~10 to 50 μm, and contains either a second phase or pores. This layer is most likely Cr_2O_3. A thinner layer that is ~5 mm thick lies below the top layer. This layer has a lighter contract that is similar to that of the base alloy. Below this layer lies another layer that is ~10 to 20 μm thick and has similar contrast to that of the top Cr_2O_3 layer. This region appears to contain large pores. Finally the bottom layer is ~15 to 20 μm thick and is consistent with internal oxidation of the alloy matrix since numerous oxide particles are present in this region.

Figure 6 shows a bright-field TEM micrograph of the microstructure observed in the ruptured specimen. This micrograph was obtained at very low magnification to show the stringers of pores. The pores have an elongated shape in the same orientation as the elongated grains in MA957 (Figure 1a). Unfortunately, the pores also prevented thin electron transparent regions from forming during electro-polishing.

(a) (b)

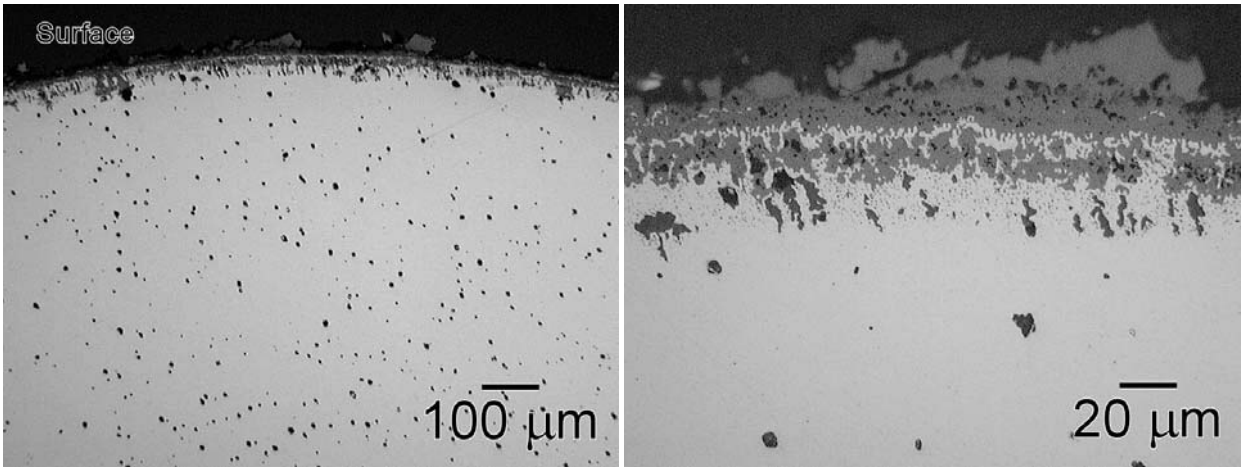

Figure 5. Optical micrographs showing the surface oxide scale and internal porosity that formed in the rupture MA957 specimen after exposure to 800ºC in air and 100 MPa load for 38,555 h. View is normal to gage of the test specimen.

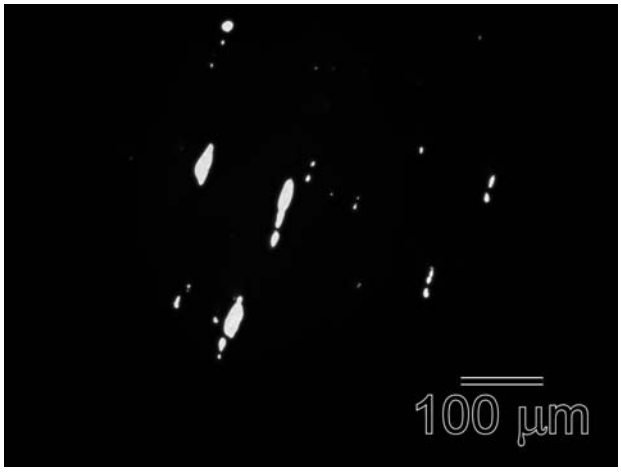

Figure 6. Bright-field TEM micrograph showing the porosity that was observed parallel the elongated grains in MA957 at a very low magnification (120 X).

Although no detailed analysis of the oxide phase in the surface scale has been conducted, this will be the focus of future research in order to investigate the possible link between the oxide scale formation and development of the porosity. Understanding these mechanisms is important since the formation of the large pores was most likely responsible for the failure mode of the creep specimen.

In order to investigate the thermal stability of the nanoclusters that were present initially in the as-received MA957 using Energy-Filtered TEM (EFTEM), which has been shown to be the most reliable electron microscopy method for imaging the nanoclusters [11], a different approach to specimen preparation was required to obtain very thin specimens. The method that finally provided the best specimen for EFTEM analysis was the lift-out method with the Focused Ion Beam (FIB) of a thin 10 μm x 10 μm specimen from the polished section of the jet-polished 3 mm dia. disc. The lift-out specimen was attached to a special grid and then thinned to electron transparency using the FIB.

The significant discovery that was obtained from the EFTEM analysis of the lift-out specimen was that the nanoclusters were still present in the ruptured specimen of MA957 and appeared to have undergone no significant change in size after 38,555 h at 800ºC and 100 MPa. Figure 7 shows 2 areas of the lift-out specimen that were analyzed using the EFTEM Fe-M jump ratio method. The results of analyzing several areas indicated that the particles showed a bi-modal size distribution and particle distribution was inhomogeneous. However, as shown in Figure 7a, the majority of the particles in the smaller size range are nanoclusters that have a size range of 2 to 4 nm. The larger particles are typically >10 nm and are usually distributed on grain boundaries, for example, the line of particles in the upper and lower region of Figure 7b. These particles are most likely an equilibrium oxide phase. However, no conclusive data was obtained that could verify this suggestion.

The results showed that the spatial distribution of the nanoclusters and larger oxide particles in the creep ruptured specimen of MA957 was relatively inhomogeneous. It was possible that this could have occurred during the creep tests. However, it was decided to have several 3 mm dia. specimens prepared from the as-received MA957 sample by jet-polishing in order to elucidate this possibility. Figure 8 shows the EFTEM Fe-M jump ratio images that were obtained from 2 regions in the as-received MA957 specimen. The results clearly showed that a bi-modal size distribution of the particles and an inhomogeneous distribution of the particles, including the nanoclusters present in the grains. Thus, these results proved that these are pre-existing characteristics of the particles dispersions in MA957 and that the nanoclusters are extremely stable very long exposures at 800ºC.

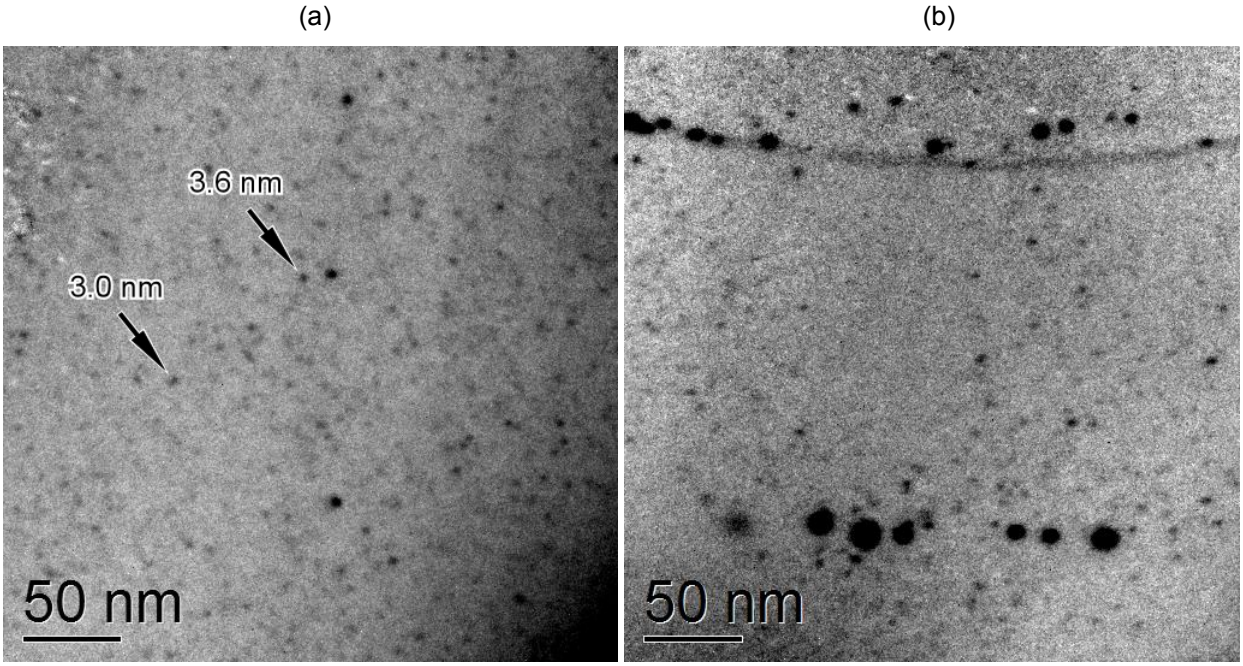

Figure 7. EFTEM Fe-M jump ratio maps of the ruptured creep specimen of MA957

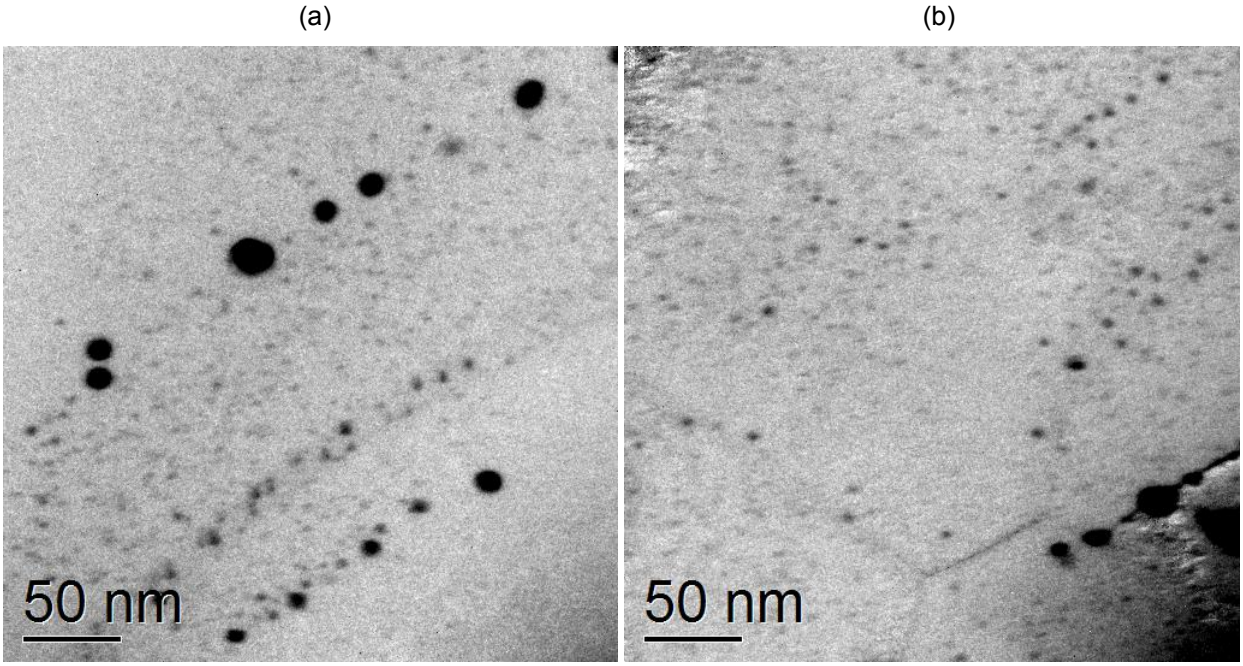

Figure 8. EFTEM Fe-M jump ratio maps of the as-received specimen of MA957.

Conclusions

- The results of the creep tests that were conducted on specimens prepared from the as-received MA7 in August 2003 showed that creep tests lasted more than 38,000 h for two of the specimens tested at

800ºC and 100 MPa and at 825ºC and 70 MPa. This was in contrast to the four specimens that were tested at temperatures between 875ºC and 925ºC with loads of either 70 MPa or 100 MPa.

- The creep results of the specimen that recently failed after 38,555 h at 800ºC and 100 MPa showed:
  - Essentially no primary or tertiary creep behavior occurred.
  - The total strain at failure was 6.5%. However, 6.14% of the strain occurred during the last 0.1 h prior to failure of the specimen, so that the steady state creep strain was only 0.361%. This corresponded to a displacement of ~0.003 in.
  - The minimum creep rate was measured to be ~1.2×10^{-11} s^{-1} ($d\dot{\varepsilon}/dt$).
- The microstructural analysis of the creep specimen that failed after 38,555 h at 800ºC and 100 MPa showed:
  - A complex multi-layer oxide scale formed on the surface of the creep specimen.
  - Extensive stringers of elongated shaped pores formed throughout the microstructure.
  - EFTEM revealed that the Ti-, Y-, O-enriched nanoclusters that were present initially in the as-received MA957 sample experienced no significant change in size, indicating that they are extremely stable at 800ºC (and 100 MPa) for very long periods of time.
  - The inhomogeneous distribution of the nanoclusters and larger oxide particles that was observed in the ruptured creep specimen was similar to that observed in specimens prepared from the as-received MA957, indicating that this was not due to the creep test conditions.

Future Work

The research that is planned for the future includes investigating the microstructure of the complex oxide scale that formed on the 800ºC creep specimen of MA957, which will involve the lift-out and FIB method for specimen preparation, and the reason for the extensive formation of porosity. The latter will include the microstructural investigation of the four creep specimens that failed with short times in the tests that were conducted at temperatures between 875ºC and 925ºC. These specimens may provide further insight into the formation of pores, stability of the nanoclusters, and specimen failure mode.

Acknowledgements

The author thanks J.R. Mayotte for the metallographic specimen preparation and D.W. Coffey and K.A. Thomas for preparing the lift-out/FIB and TEM thin foil specimens, respectively. This research was supported by the Office of Nuclear Energy, Science and Technology (INERI), by the Office of Fusion Energy Sciences, and at the SHaRE User Facility by the Scientific User Facilities Division, Office of Basic Energy Sciences, U.S. Department of Energy.

References

[1] J.J. Fisher, US Patent 4,075,010, issued 21 February 1978.
[2] M.K. Miller, D.T. Hoelzer, E.A. Kenik, and K.F. Russell, J. Nucl. Mater., Vol. 329-333 (2004) p. 338.
[3] M.J. Alinger, PhD Dissertation, University of California, Santa Barbara, September 2004.
[4] D.J. Larson, P.J. Maziasz, I.-S. Kim, and K. Miyahara, Scr. Mater., Vol. 44 (2001), p. 359.
[5] I.-S. Kim, B.-Y Choi, C.-Y Kang, T. Okuda, P.J. Maziasz, and K. Miyahara, ISIJ International, Vol. 43, No. 10, (2003), p. 1640.
[6] M.K. Miller, Atom Probe Tomography, Kluwer Academic/Plenum, New York, 2000.

[7] M. Brady, B. Gleeson, and I.G. Wright, JOM, Vol. 52, No. 1 (2000), p. 16.
[8] R.L. Klueh, P.J. Maziasz, I.S. Kim, L. Heatherly, D.T. Hoelzer, N. Hashimoto, E.A. Kenik, and M. Miyahara, J. Nucl. Mater., Vol. 307-311 (2002), p. 773.
[9] Z.Y. Gao, F.S. Han, J. Wu, and Q.Z. Wang, J. Alloys and Compounds, Vol. 419, (2006), p. 126.
[10] B.A. Pint and I.G. Wright, Oxidation of Metals, Vol. 63, No. 3-4 (2005), p. 193.
[11]. J. Bentley, D.T. Hoelzer, D.W. Coffey and K.A. Yarborough, Microsc. Microanal., Vol. 10 (Suppl. 2), (2004), p. 662.